Effect of Diamide on Force Generation and Axial Stiffness of the Cochlear Outer Hair Cell

M. Adachi and K. H. Iwasa
Biophysics Section, Laboratory of Cellular Biology, National Institute on Deafness and Other Communication Disorders, National Institutes of Health, Bethesda, Maryland 20892-0922 USA

ABSTRACT We found that diamide, which affects spectrin, reduces the axial stiffness of the cochlear outer hair cell, the cylindrically shaped mechanoreceptor cell with a unique voltage-sensitive motility. This effect thus provides a means of examining the relationship between the stiffness and the motility of the cell. For measuring axial stiffness and force production, we used an experimental configuration in which an elastic probe was attached to the cell near the cuticular plate and the other end of the cell was held with a patch pipette in the whole-cell recording mode. Diamide at concentrations of up to 5 mM reduced the axial stiffness in a dose-dependent manner to 165 nN per unit strain from 502 nN for untreated cells. The isometric force elicited by voltage pulses under whole-cell voltage clamp was also reduced to 35 pN/mV from 105 pN/mV for untreated cells. Thus the isometric force was approximately proportional to the axial stiffness. Our observations suggest a series connection between the motor and cytoskeletal elements and can be explained by the area motor model previously proposed for the outer hair cell.

INTRODUCTION

The outer hair cell (OHC) has a unique motility which is considered important for the normal function of the ear (Brownell et al., 1985; Ashmore, 1987). The importance of this motility has been demonstrated both in vivo (Xue et al., 1993) and in isolated cochleas (Mammano and Ashmore, 1993). Unlike most other biological motilities, this membrane-potential-dependent motility is not dependent on ATP, the usual source of chemical energy (Kachar et al., 1986; Holley and Ashmore, 1988). The motor mechanism responsible for the motility is located in the plasma membrane of the lateral wall (Dallos et al., 1991; Kalinec et al., 1992; Huang and Santos-Sacchi, 1994) and uses electrical energy. The membrane motor has at least two conformational states, and charges are transferred across the membrane during transitions between these states. These charge transfers are observed as the voltage dependence of the membrane capacitance (Ashmore, 1990; Santos-Sacchi 1991; Iwasa, 1993). Moreover, this capacitance is also dependent on cell pressure delivered through a patch pipette in the whole-cell recording configuration (Iwasa, 1993; Gale and Ashmore, 1994; Kakehata and Santos-Sacchi, 1995). Thus the state of the motor is dependent not only on the membrane potential, but also on membrane tension, demonstrating direct electromechanical coupling in the membrane motor (Iwasa, 1993, 1994).

These observations also imply that the stiffness of the membrane is critically important for force production in this cell (Iwasa and Chadwick, 1992; Iwasa, 1994). It is likely that the stiffness of the cell depends on the cytoskeletal undercoating, because the membrane stiffness of this cell is lower than that of a lipid bilayer (Iwasa, 1996; Bloom et al., 1991). Moreover, the characteristic cylindrical shape of this cell membrane must be supported by a cytoskeletal undercoating of the lateral plasma membrane (Holley, 1996). The structure underlying the lateral membrane of the OHC is extensive, consisting of the cortical lattice, the pillar structure that connects the plasma membrane with the cortical lattice, and an extensive submembranous cysternae system (Kalinec et al., 1992; Holley, 1996). The known constituents of the cortical lattice include actin, spectrin, and protein 4.1 (Knipper et al., 1995).

Diamide (azodicarboxylic acid bis[dimethyamide]) is a membrane-permeable sulfhydryl reagent that affects spectrin (Kosower and Kosower, 1995). Its effect has been extensively studied in erythrocytes (Haest et al., 1977; Maeda et al., 1983; Becker et al., 1986). Diamide treatment of the OHC makes the cell highly extendable, but it does not have a significant effect on the motility of the cell under the load-free condition (Kalinec and Kachar, 1993). These observations are suggestive that diamide may have a significant effect on the axial stiffness of the cell without a significant effect on the membrane motor. The method we have developed for measuring the axial stiffness and force production of the cell under voltage clamp (Iwasa and Adachi, 1997) should be useful for examining the relationship between the membrane stiffness and force production in the OHC.

In this paper, we examine the effect of diamide on the axial stiffness of the OHC under voltage clamp. The membrane-potential-dependent force production in the same cells is determined by applying voltage pulses from the patch pipette. We supplement these observations with length changes elicited by voltage changes in the load-free

Received for publication 19 March 1997 and in final form 30 July 1997.

Address reprint requests to Dr. Kuni H. Iwasa, Biophysics Section, Cellular Biology Laboratory, National Institute on Deafness and Other Communication Disorders, Rm. 1E120, Bldg. 9, National Institutes of Health, 9 Center Dr., MSC 0922, Bethesda, MD 20892-0922. Tel.: 301-496-3987; Fax: 301-480-0827; E-mail: kiwasa@helix.nih.gov.

0006-3495/97/11/2809/10 $2.00

condition. The experimental data obtained are analyzed based on the two-state membrane motor model (Iwasa, 1994), extended to incorporate mechanical orthotropy instead of mechanical isotropy (Iwasa and Adachi, 1997).

MATERIALS AND METHODS

Cell preparation

Bullas were obtained from guinea pigs. The organ of Corti was dissociated from opened cochleas by teasing with a fine needle under a dissection microscope. The strips of organ of Corti thus obtained were tritulated three times gently with a plastic pipette and placed in a chamber mounted on an inverted microscope. The lengths of the cells used for the experiment ranged between 40 μm and 75 μm. For experiments that use fiber probes, clusters of OHCs, preferably formed by two or three cells, connected at their apical ends were chosen. For experiments to observe load-free movements, isolated cells were chosen. In some of the experiments in the load-free condition, dispase (Boehringer-Mannheim) treatment (0.5 units/ml for 20 min at 21°C) was used before mechanical isolation.

Chemical treatment of the cells

Diamide (Sigma) was dissolved in the bath medium, which contained 135 mM NaCl, 5 mM KCl, 2 mM $MgCl_2$, 1.5 mM $CaCl_2$, 5 mM glucose, and 10 mM HEPES. The diamide concentrations were between 1 mM and 5 mM. Cells were incubated in these media for 30 min at 21°C. After the incubation, the media were replaced by the regular bath medium. Experiments were performed on the treated cells within 60 min after washout.

Probes

The method of manufacturing the fiber probes was described earlier (Iwasa and Adachi, 1997). Glass capillaries (1.5 mm O.D.) were pulled with a BB.CH.PC puller (Mechanex, Switzerland) to form fine fibers near the tip. These glass capillaries could be used as probes after their bending stiffnesses at the tip were calibrated. The calibration procedure involves bending a probe near the tip with a glass fiber with known stiffness under a microscope. As the primary standard, a relatively long and thick glass fiber was pulled by hand and cut to make a piece 5 cm long. After one end of the thick fiber was fixed to a glass capillary with epoxy glue, its bending stiffness at the other end was determined by measuring the displacement under a microscope while a number of thin, short platinum wires with known mass (between 0.1 and 1 mg) were hung near the tip. To facilitate calibrating the probe used for the experiments, a secondary standard with a smaller diameter was used. This procedure was similar to the method described by Kojima et al. (1994). The fiber probe used had a stiffness of 4.6 nN/μm.

Patch clamping

Patch pipettes were fabricated by pulling glass capillaries (blue tip) with a BB.CH.PC puller (Mechanex, Switzerland). The pipette resistance was between 1.5 and 2.5 MΩ when filled with an intracellular medium. The cells that showed a zero-current potential more negative than -50 mV were used for the experiment. The access resistance was between 3 and 5 MΩ. The imput impedance of the cells used was between 40 and 100 MΩ. This description applies to both untreated cells and diamide-treated cells. The internal medium contained 145 mM KCl, 2 mM $MgCl_2$, 1 mM EGTA, 0.555 mM $CaCl_2$, and 10 mM HEPES. The external medium contained 135 mM NaCl, 5 mM KCl, 2 mM $MgCl_2$, 1.5 mM $CaCl_2$, 5 mM glucose, and 10 mM HEPES. The pH of both media was adjusted to 7.4. Osmolarity was adjusted to 300 mOsm/kg with glucose. A patch amplifier (EPC-7; List Electronic, Darmstadt, Germany) was used for whole-cell voltage-clamp experiments. A train of voltage pulses was generated with an ITC-16 interface (Instrutech, Great Neck, NY) on a computer using the Synapse program (Synergistic Research, Silver Spring, MD).

Determination of stiffness

A fiber probe was placed at an extension of the cuticular plate connecting two or three outer hair cells. The contact point is basal to the connecting structure, so that the cell can be pulled. This configuration did not allow us to apply a compressive force to the cell with the fiber probe, because moving the probe in the opposite direction could disengage the contact. A tight seal was then formed with a patch pipette on one of the cells at the lateral wall near the basal end, but more apical than the nucleus. The system was brought to whole-cell configuration by applying a train of brief pulses across the electrodes (zapping). External tension was applied to the cell by stretching it with the patch pipette while holding the other end with the fiber probe (Fig. 1).

To mark fixed positions on the cell membrane, polyacrolein microspheres 1 μm in diameter (Polysciences, Warrington, PA) were introduced to the external bath. Five microliters of microspheres was prediluted into 1 ml of the bath medium, and then 40 μl of the suspension was added to the chamber containing the 200 μl of bath medium (Zajic and Schacht, 1991). Microspheres attached to the surface of the cell were used for determining the axial strain of the cell.

Images of the cell with the fiber probe were stored with a video recorder and digitized off-line with an image grabber card (Scion, Frederick, MD), using a computer program (National Institutes of Health Image, W. Rasband, NIMH). The accuracy in determining the position of the probe and the axial strain of the cell was enhanced by fitting the light intensity peaks that corresponded to the probe, microspheres, and cell edges with a parabola. The number of points used for the fit was usually five. The process was automated by developing a macro for the National Institutes of Health Image program.

Movement under an elastic load

In the same configuration as was used for determining the axial stiffness, voltage pulses were delivered to the cell from the patch electrode. To

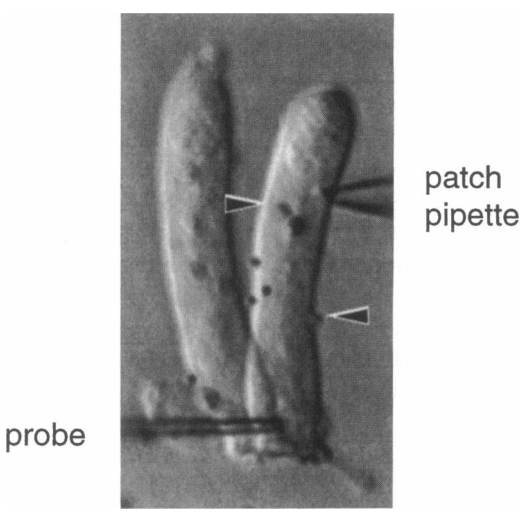

FIGURE 1 Photomicrograph showing the configuration for monitoring the axial force of the outer hair cell. The whole cell patch is formed on the lateral membrane slightly apical to the nucleus. The fiber probe is attached to a link connecting two outer hair cells, so that tension can be applied to the cell. Micospheres (*arrows*) attached to the lateral membrane serve as markers for determining the axial strain.

ensure that the OHC was kept under tension, the holding membrane potential was usually set at −80 mV or at a slightly more negative value (see Results). The durations of the applied voltage pulses were between 100 ms and 1 s, to keep them compatible with the video rate. The microscope images of the cell and the probe were stored with a video recorder and analyzed off-line in a manner similar to that of the stiffness determination described above.

Cell movement under load-free condition

A wide range of the membrane potential was used under the load-free condition to determine the maximum amplitude of length changes. To avoid inducing large jerky movements of the cell, which tend to destroy the whole-cell recording configuration, voltage ramps were applied from the patch electrode. In some experiments, the same pulses used for force measurements were used. The microscope images of the cell were stored with a video recorder and analyzed off-line.

RESULTS

The axial stiffness

After the system was brought to the whole-cell recording configuration, the cell was stretched with the patch pipette. The force applied to the cell was measured with a stationary fiber probe, which held the cell at an extension of the cuticular plate (Fig. 1). The strain of the cell membrane was determined based on the distance between the cuticular plate and microspheres. The microspheres chosen were attached to the lateral wall between the cuticular plate and the patch pipette. The axial stiffness of the cell was described as the force per unit axial strain (Fig. 2). The mean axial stiffness obtained was 502 nN per unit strain in the control condition, consistent with the previous report (Iwasa and Adachi, 1997). The holding potential was −80 mV. The strain applied was less than 0.1, and was typically near 0.04.

Diamide-treated cells showed reductions in the axial stiffness (Table 1, Fig. 3). The effect was concentration dependent. The reduction of the stiffness was 24% at 1 mM, 39% at 2 mM, and 67% at 5 mM. Data for concentrations higher than 5 mM were not obtained because we could not maintain the whole-cell recording mode on those cells treated at higher concentrations.

In some cases diamide-treated cells could be stretched several times the original length. We were unable to determine whether the elasticity remains linear in these instances, because microspheres on the membrane went out of the field.

Force generation

To determine the axial stiffness, we moved the patch pipette to stretch the cell. Then the pipette was kept stationary while a train of depolarizing voltage pulses was applied. The voltage pulses elicited cellular motility, bending the force probe (Fig. 4). The response was approximately linear to the amplitude of applied pulses. The holding potential was −80 mV to avoid length changes due to imposing a holding potential (Iwasa, 1996; Iwasa and Adachi, 1997). Hyperpolarizing pulses were not applied, because an elongation of the cell from the resting position may reduce the coupling between the probe and the cell. The force directly detected by the probe may reflect characteristics of the cell, but it also depends on various experimental factors such as the stiffness of the probe and the distance between the patch pipette and the probe. To compensate for these factors we use a formula:

$$f_{\text{isometric}} = (k_p + K_c L^{-1})\Delta z, \quad (1)$$

to obtain an extrapolation to isometric force $f_{\text{isometric}}$, where k_p is the stiffness of the probe (per unit displacement), L is the distance between the patch pipette and the apical end of the cell where the probe is attached, K_c is the axial stiffness of the cell (per unit strain), and Δz is the displacement of the probe (Iwasa and Adachi, 1997). The physical meaning of Eq. 1 will be examined after we derive Eq. 7.

Cells in the control condition produce 100 pN/mV, as in the previous study. Diamide-treated cells show reduced force production for a given amplitude of voltage pulses (Fig. 5 *A*). Because the force elicited was approximately linear to the voltage amplitude, the average slope was used to plot against diamide concentration (Fig. 5 *B*). The slope reduction from the control is 25% at 1 mM, 55% at 2 mM, and 66% at 5 mM. The relative reduction in force generation

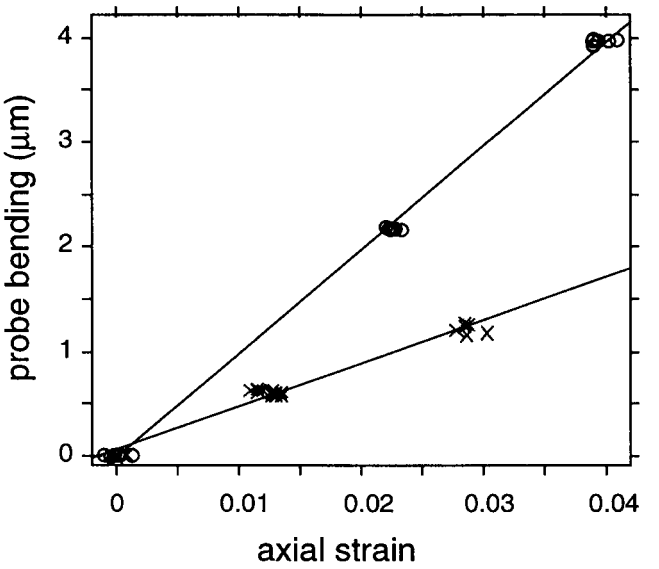

FIGURE 2 Determination of the axial stiffness. Axial strains are determined based on distances between the cuticular plate and microspheres attached to the lateral wall. Cells are pulled in two steps. An untreated cell (○) with natural length 72.9 μm and a cell treated with 5 mM diamide (×) with natural length 53.1 μm are shown. The distance before stress is 48.9 μm for the untreated cell and 44.3 μm for the diamide-treated cell. The best fits (*solid lines*) give 99 μm/strain and 41 μm/strain, respectively, for the untreated cell and the one treated with 5 mM diamide. Given 4.6 nN/μm of the probe stiffness, the axial stiffness of the untreated cell is 457 nN/strain, and the stiffness of the cell treated with 5 mM diamide is 189 nN/strain. Sampling is at 333-ms intervals for the untreated cell and 300 ms for the treated cell.

TABLE 1 The axial stiffness, force detected by the probe, and isometric force produced by the outer hair cell

Diamide conc. (mM)	Axial stiffness (nN)	Bending of probe (nm/mV)	Force at probe (pN/mV)	Est. isometric force (pN/mV)	N
0	502 ± 22	6.75 ± 0.72	31 ± 3	104 ± 17	8
1	381 ± 19	5.82 ± 0.73	27 ± 3	78 ± 7	5
2	306 ± 9	4.09 ± 0.28	19 ± 1	47 ± 7	5
5	165 ± 20	3.84 ± 0.67	17 ± 7	35 ± 8	5

The probe used had a stiffness of 4.6 nN/μm. The values given are means ± standard error.

due to diamide is similar to the relative reduction of the axial stiffness.

Movement under load-free condition

Length changes of the cell due to changes in the membrane potential were examined with isolated OHC. A polystyrene-bottomed chamber (CoverWell; Grace Biolabs, Sunriver, OR) was used for this experiment to reduce friction. To determine the saturating amplitude of length changes, we used ramps between −150 mV and +105 mV. This voltage waveform was advantageous in maintaining the whole-cell configuration, because it does not elicit jerking motion. The axial strains due to voltage changes are highly reproducible (Fig. 6) and were consistent with data obtained with short pulses in a narrower range. To obtain the value for the saturating amplitude of length changes, we attempted to fit the length-voltage plot with a two-state Boltzmann function:

$$\epsilon_z = \frac{\Delta\epsilon}{1 + \exp[q^*(V - V_0)]},$$

where $\Delta\epsilon$ is the saturating amplitude of length change, and V_0 is the voltage of the steepest slope. The quantity q^* is the steepness parameter of the transition and is related to the gating charge q by $-q/k_BT$, where k_B is Boltzmann's constant and T is the temperature.

Diamide increased the saturating amplitude of voltage-dependent length changes on the average. For control cells, the mean saturating amplitude $\Delta\epsilon$ was 4.88% of the cell length. Diamide increases the amplitude by up to ~40% (Table 2).

This increase of amplitude due to diamide was accompanied by a shift of the voltage of the steepest slope. Whereas the voltage V_0 of the steepest slope was on the average −26.7 mV for control cells, it was −65 mV at 5 mM

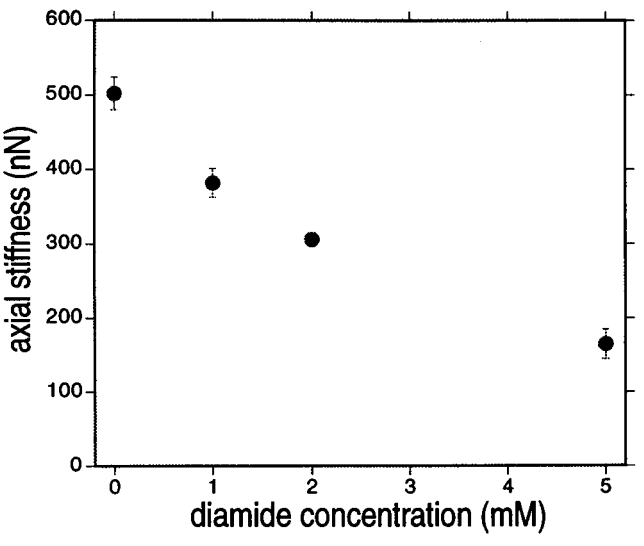

FIGURE 3 Dependence of the axial stiffness of the OHC on diamide concentration. The axial stiffness is determined as force divided by axial strain while the patch pipette pulled the cell for 0.2 s. The holding potential is −80 mV. Bars indicate standard errors.

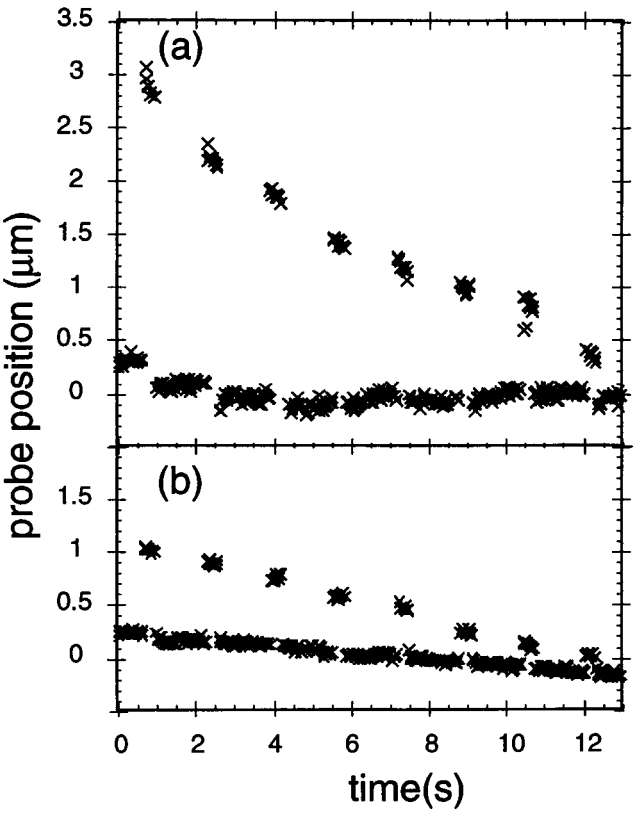

FIGURE 4 Bending of the probe elicited by voltage pulses. The amplitude of the fist depolarizing pulse applied is 100 mV, and the amplitudes of consecutive pulses are reduced by 10 mV. The holding potential is −80 mV. (*a*) Untreated cell with natural length 74.1 μm; (*b*) cell treated with 2 mM diamide with natural length 42.3 μm. The separation between the patch pipette and the fiber probe is 61.1 μm for the untreated cell and 32.4 μm for the treated cell. Sampling is at 33.3-ms intervals. Probe bending is measured from the baseline. The stiffness of the probe is 4.6 nN/μm.

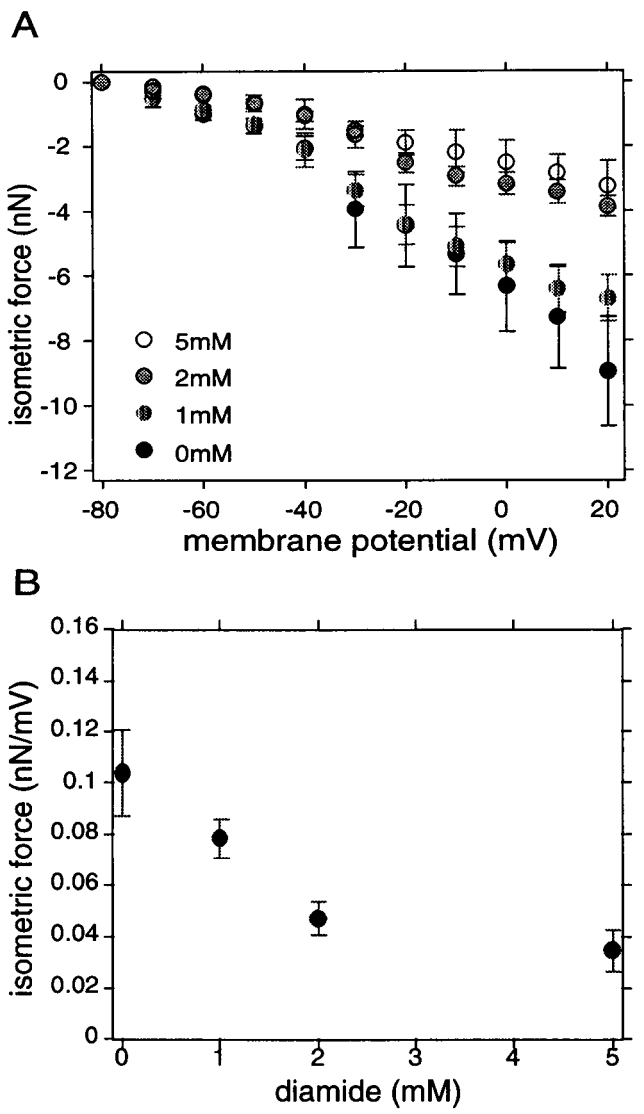

FIGURE 5 Isometric force elicited by voltage pulses. Isometric force is obtained as an extrapolation with the formula $(K_c/L + k_p)\Delta z_p$, where K_c is the axial stiffness of the cell (per unit strain), k_p is the stiffness of the probe (per unit distance), Δz_p is the probe displacement, and L is the separation between the probe and the patch pipette. The holding potential was −80 mV. The duration of the pulses was 300 ms. (*A*) Isometric force elicited by membrane potential pulses. *Filled circles*, Control; *striped circles*, 1 mM; *gray circles*, 2 mM; *open circles*, 5 mM diamide. Bars indicate standard errors. (*B*) Dependence of isometric force generation on diamide concentration. Force generation was plotted as the absolute value of force per millivolt. Bars indicate standard errors.

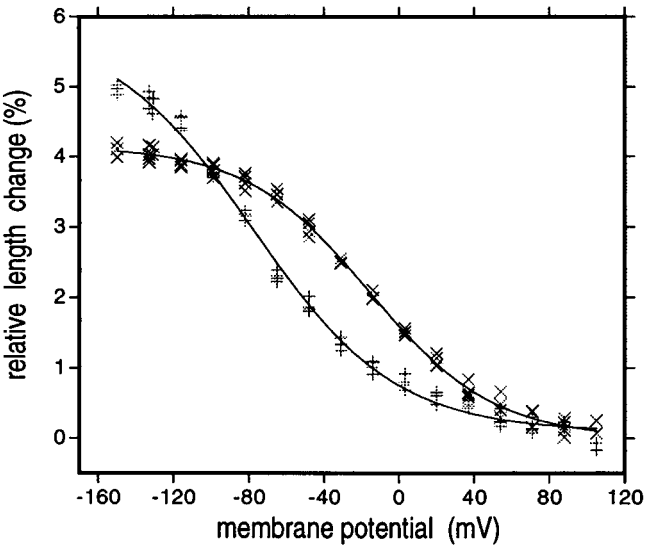

FIGURE 6 Examples of membrane potential dependence of the relative cell length. Response to repeated voltage ramps, going between −150 mV and 105 mV in 1 s. +, 3 mM diamide; ×, control. The holding potential is −75 mV. The total length of the cell was used for the plot. The cell length at the holding potential is 61.5 μm for the control cell and 53.7 μm for the treated cell.

diamide. These changes were accompanied by changes in the sharpness q^* of the transition (Table 2).

DISCUSSION

Modification of stiffness by diamide

It has been shown that oxidation of sulfhydryl groups in diamide results in increasing intermolecular links between spectrin molecules in the erythrocytes, resulting in hardening of the cell (Haest et al., 1977; Maeda et al., 1983). However, diamide reduces actin binding of spectrin mediated by protein 4.1 (Becker et al., 1986).

The observed stiffness change in the OHC appears to reflect the change in the cytoskeletal undercoating of the lateral wall. The major components of the cytoskeleton that support the lateral wall of the OHC consist of actin filaments (Holley et al., 1992), spectrin (Holley and Ashmore, 1990; Nishida et al., 1993), protein 4.1 (Knipper et al., 1995), and pillars (Flock et al., 1986), forming a relatively regular structure, which is usually referred to as the cortical lattice (Holley, 1996). Actin filaments run parallel to each other, primarily in the circumferential direction. The structure that connects these actin filaments presumably consists of spectrin (Holley, 1996). Protein 4.1 is thought to link spectrin and actin filaments, and spectrin is oriented in the axial direction, linking actin filaments. The effect of diamide in weakening actin binding of spectrin should result in a reduction in the stiffness of the cortical lattice. Our result

TABLE 2 Motility parameters of the outer hair cell in the load-free condition

Diamide conc. (mM)	Saturating amplitude (%)	Midpoint potential (mV)	Apparent charge (e)	N
0	4.88 ± 0.27	−26.7 ± 2.7	0.76 ± 0.04	14
1	5.32 ± 0.23	−39.9 ± 5.5	0.69 ± 0.03	6
3	5.43 ± 0.43	−63.9 ± 9.3	0.65 ± 0.02	7
5	6.95 ± 0.64	−64.7 ± 7.8	0.65 ± 0.04	5

The values given are means ± standard error. The apparent charge q is related to the sharpness q^* of the transition by $q^* = -q/k_BT$. It is expressed in electronic charge e. The value for this quantity in untreated cells is consistent with the values determined by capacity measurements.

indicates that the cortical lattice is critically important in determining the axial stiffness of the cell.

The stiffness of untreated cells is consistent with our previous report (Iwasa and Adachi, 1997), and a detailed comparison with earlier reports has been given there. The value of 502 nN per unit strain lies between the mean value (200 nN) and an upper bound (750 nN) reported by Hallworth (1995). As we have reported previously (Iwasa and Adachi, 1997), the axial stiffness is virtually independent of cell length if the stiffness is described in terms of force per unit strain. This unit is thus advantageous in describing the effect of diamide on the stiffness.

Description of the system by the area motor model

Here we will examine how changes in the axial stiffness of the cell affect the electromotility of the OHC based on the area motor model. This model was initially proposed for isotropic cell membrane (Iwasa, 1994) and then extended by incorporating mechanical orthotropy (Iwasa and Adachi, 1997). The basic assumptions of this model are that 1) the electromotility is based on a membrane motor that changes the membrane area it occupies and that 2) the motor and the elastic elements are connected in series. Because the motor mechanism is based on area changes, as opposed to stiffness changes, the model is called the "area motor" model (Iwasa, 1997).

The OHC is approximated by a cylinder of radius r. We also assume that the OHC is elastic. This assumption is expected to be adequate for describing displacements of the cell for durations not exceeding several seconds (Ehrenstein and Iwasa, 1996), such as in the present experimental conditions. Tension T_z in the axial direction and tension T_c in the circumferential direction due to elastic strains ϵ_z' (axial direction) and ϵ_c' (circumferential direction) are balanced by the force exerted by internal pressure p and an axial tension T_x due to an externally applied axial force,

$$\begin{aligned} d_z\epsilon_z' + c\epsilon_c' &= T_z = \tfrac{1}{2}rp + T_x, \\ c\epsilon_z' + d_c\epsilon_c' &= T_c = rp, \end{aligned} \tag{2}$$

where d_z is a diagonal element of the elastic tensor relating an axial stress with the axial strain ϵ_z', d_c is the other diagonal element relating the stress in the circumferential stress to the strain ϵ_c' in the circumferential direction, and c is the off-diagonal element. Equation 2 is based on mechanical orthotropy (Tolomeo and Steele, 1995; Iwasa and Adachi, 1997). As in a previous treatment (Iwasa, 1994), we assume that the total strains ϵ_z and ϵ_z are represented by sums of the elastic strains and motor strains, i.e.,

$$\epsilon_z = \epsilon_z' + nP_1a_z \quad \text{and} \quad \epsilon_c = \epsilon_c' + nP_1a_c. \tag{3}$$

Here n is the (number) density of the motor in the lateral membrane, a_z is the axial component of the area change of the motor, and a_c is the circumferential component. The probability that the motor is in the extended state is represented by P_1,

$$\frac{P_1}{1-P_1} = \exp\left[-\frac{\Delta F}{k_BT}\right] \tag{4}$$

with the free energy difference of the motor in the two states,

$$\Delta F = F_0 + qV + (a_zT_z + a_cT_c) \tag{5}$$

where F_0 is a constant, q is the charge transferred across the membrane during transitions between the two states, and V is the membrane potential. The Boltzmann constant and the temperature are respectively represented by k_B and T. The external tension T_x can be related to the axial strain of the cell ϵ_z,

$$T_x = \frac{k_pL^*}{2\pi r}\epsilon_z, \tag{6}$$

because the elastic force of the probe is $k_p\Delta z$ for a displacement Δz, and the length of the cell is L^*. The tension T_x due to the probe is applied throughout the cell. In our experimental configuration, the cell is not held at the basal end but at the lateral wall (Fig. 1) somewhat above the nucleus, because we found that the basal part of the cell is softer than the rest (Iwasa and Adachi, 1997). For our experimental condition, L^* should be replaced by L, the resting distance between the patch pipette and the cuticular plate where the fiber probe is attached. Not subjecting the whole lateral membrane to tension reduces changes in the pressure p. For this reason our model gives a better description of longer cells, where the relative differences between L and L^* are smaller.

It is reasonable to assume that the volume of the cell is constant for responses to changes in the membrane potential (Iwasa and Chadwick, 1992). This condition, $\epsilon_z + 2\epsilon_c = \epsilon_{v0}$, reduces the number of variables. Here ϵ_{v0} is the volume strain in the standard membrane potential. With Eqs. 2, 3, and 6, the axial strain is given in the form

$$(K_c + Lk_p)\epsilon_z = 2\pi r(a + bP_1). \tag{7}$$

Here K_c is the axial stiffness of the cell. The left-hand side of Eq. 7, which is equivalent to Eq. 1, is force produced by the cell. The quantities a and b are constants. They are represented by

$$\begin{aligned} K_c &= 2\pi r(d_z - c + \tfrac{1}{4}d_c), \\ a &= -\tfrac{1}{2}(c - \tfrac{1}{2}d_c)\epsilon_{v0}, \\ b &= \tfrac{1}{2}[(2d_z - c)a_z + (2c - d_c)a_c]. \end{aligned} \tag{8}$$

In the limit of infinite k_p, the left-hand side of Eq. 7 represents isometric force. The probability P_1 of the extended state is dependent on the membrane potential V as well as the stress, as Eqs. 4 and 5 show. Because the quantity P_1 is not sensitive to the probe stiffness k_p, as shown in a previous paper (Iwasa and Adachi, 1997), the

left-hand side of Eq. 7 is a good approximation for isometric force.

The pressure-strain relationship (Iwasa and Chadwick, 1992) of untreated cells gives $\epsilon_z P = -69 \times 10^{-6}\ P^{-1}$ and $\epsilon_c/P = 130 \times 10^{-6}\ P^{-1}$. The axial stiffness, which is represented by $2\pi r(d_z - c + \frac{1}{4}d_c)$, has a value of 500 nN per unit strain. The radius r of the cell is usually 5 μm. Using these conditions with Eq. 2 under voltage clamp, we obtain the values for elastic moduli for untreated cells. They are $d_z = 45.9$ mN/m, $c = 46.2$ mN/m, and $d_c = 68.0$ mN/m. The pressure dependence of the membrane capacitance imposes a condition for motor displacement. It is between 3 and 4 nm^2 for the quantity $2(a_z + 2a_c)/3$ (Iwasa, 1993). The amplitude of load-free motility imposes a condition for the ratio of a_z to a_c. To make the amplitude ~4.5% of the cell length, we set $a_z = 10$ nm^2 and $a_c = -2$ nm^2.

The effect of diamide appears to weaken the bonds between spectrin and actin filaments, which are mediated by protein 4.1. Actin filaments in the lateral wall are primarily in the circumferential direction, and spectrin links between these filaments are approximately in the axial direction. Although the relationship between cytoskeletal undercoating of membrane and the mechanical properties of the membrane may not be simple, it could be reasonable to assume that the modulus d_z decreases by diamide treatment. Indeed, a reduction in the modulus d_z is effective in reducing the axial stiffness of the cell.

An additional condition on the elastic moduli can be obtained by examining osmotic responses of diamide-treated OHCs. A preliminary study indicates that the ratio ϵ_c/ϵ_z during hypoosmotic perfusion for the cells treated with 5 mM diamide is approximately -1.5, whereas it is -1.9 for untreated cells. If we assume that the reduction in the axial stiffness by as much as 66% (5 mM) is due solely to a change in the modulus d_z, the ratio ϵ_c/ϵ_z must be about -1.0 for the cells treated with 5 mM diamide. This is easily shown with Eq. 1 by ignoring the effect of the motor, because for relatively large displacements, the motor is not important (Iwasa, 1994). Thus this observation is not compatible with the interpretation that the axial modulus d_z alone is responsible for the changes due to diamide.

Because actin filaments, which are not directly modified by diamide, are approximately perpendicular (deviation of ~15°) to the axis of the cell (Holley, 1996), it is likely that the modulus d_c does not undergo significant changes. We assumed somewhat arbitrarily that the relative reduction in the circumferential modulus d_c is small and proportional to the dose and 6.7% at 5 mM, one-tenth of the 67% reduction for the axial stiffness. We then determined d_z and c to satisfy the conditions for the axial stiffness and those for the strain ratio ϵ_c/ϵ_z during hypoosmotic perfusion. With these conditions we obtain for the diamide-modified elastic moduli (d_z, d_c, c) a set of values (36.5, 59.1, 39.2) (mN/m) at 1 mM, (32.2, 58.1, 37.3) at 2 mM, and (24.9, 56.5, 33.6) at 5 mM, whereas the set for untreated cells is (45.9, 68.0, 46.2). These sets satisfy the condition $d_z d_c > c^2$ for orthotropy (Iwasa and Chadwick, unpublished results). We examined the effect of different assumptions on the modulus d_c and found that the result was not very sensitive to the assumption on the circumferential modulus d_c. As would be clear from Eq. 8, the axial stiffness K_c is primarily determined by the difference between the axial modulus d_z and the cross-modulus c. If the cross-modulus decreases less than the axial modulus d_z, the axial stiffness K_c decreases much more steeply than d_z, as the above example shows.

Bending of elastic probe

The stiffness of the probe used was 4.6 nN/μm. The theoretical model was evaluated, assuming that the cell length is 60 μm, about the average length of the cells used. A reduction in the axial stiffness brings about a reduction in probe displacements (*solid lines*) similar to that in experimental observations (*broken lines*) (Fig. 7 *A*). Although this plot is useful in examining the validity of the theory, it is not very useful in characterizing the cellular property, because it depends on the stiffness of the probe. It has been shown that the cellular force measured with a stiffer probe is larger (Iwasa and Adachi, 1997).

Isometric force

Isometric force is the force detected by an infinitely stiff probe. The magnitude of isometric force (100 pN/mV) for untreated cells is consistent with our previous value (Iwasa and Adachi, 1997). As discused in the previous paper, this value is larger than earlier estimates from isolated cells, with a mean value of 20 pN/mV and a maximum of 70 pN/mV (Hallworth, 1995). It is, however, smaller than the 200 pN/mV estimated from in vivo data (Xue et al., 1993, 1995).

According to Eq. 7, the saturating amplitude of isometric force due to voltage changes is proportional to b, which is defined by Eq. 8. Because the motor area change a_z in the axial direction is positive and more important than the change a_c in the circumferential direction, a reduction in the elastic modulus d_z due to diamide results in decreasing b. Thus there is a reduction in d_z, leading to reduced force production (Fig. 7 *B*). The numerical examination (Fig. 8) indeed shows that the axial stiffness and isometric force are approximately proportional. The result is consistent with our experimental data. In the voltage range (betweeen -80 mV and 20 mV) examined to obtain isometric force, the length change in the load-free condition is relatively constant with respect to diamide concentration (Fig. 6). For this reason, the voltage shift cannot be a major factor in reducing the isometric force with increasing diamide concentration.

The reason we obtained an increase in the axial stiffness associated with an increase in force generation is that our model is based on a series connection between the motor element and the elastic element. This result is inconsistent with a parallel connection.

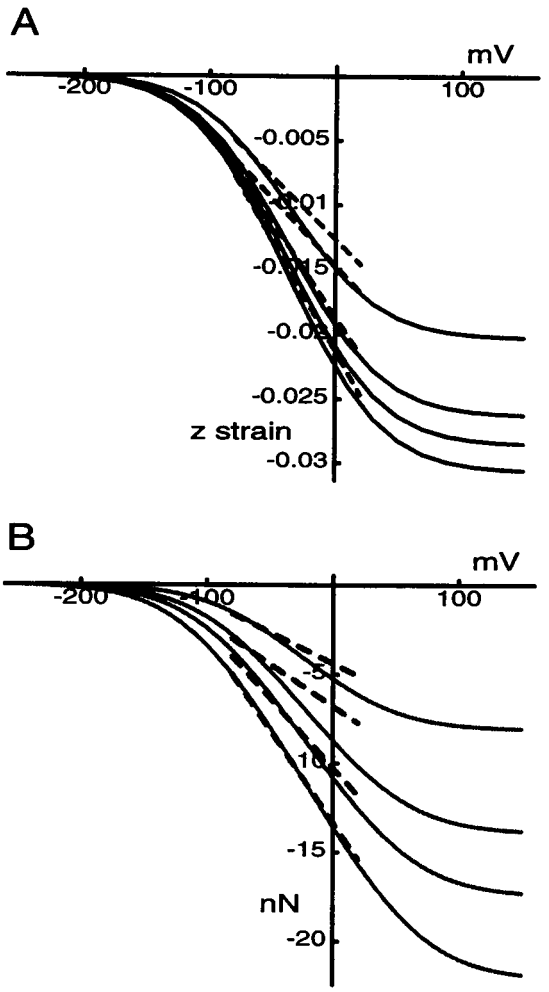

FIGURE 7 Theoretical predictions of the two-state area motor model on the effect of reduced stiffness due to diamide. Parameter values: radius r of the cell, 5 μm; length of the cell, 60 μm; q = 0.8e (electronic charge); number N of the motor in the cell, 7×10^6; a_z = 10 nm^2; a_c = -2 nm^2. The elastic moduli (d_z, d_c, c) have a set of values (36.5, 59.1, 39.2) (mN/m) at 1 mM, (32.2, 58.1, 37.3) at 2 mM, and (24.9, 56.5, 33.6) at 5 mM. The set for untreated cells is (45.9, 68.0, 46.2). See text for details. (*A*) Probe bending plotted against the membrane potential. ——, Theoretical prediction. – – –, Experimental slope. From the top trace, 5 mM, 2 mM, 1 mM diamide, and control (*bottom*). The probe stiffness is 4.6 nN/μm. (*B*) Isometric force generated by the cell plotted against the membrane potential. ——, Theoretical prediction. – – –, Experimental slope. From the top trace, 5 mM, 2 mM, 1 mM diamide, and control (*bottom*).

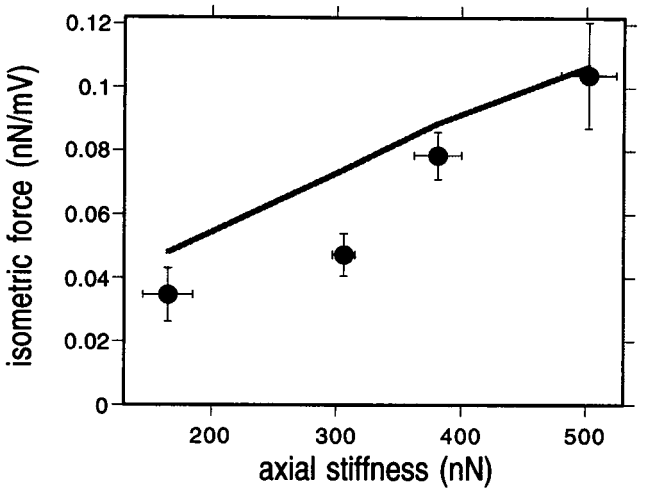

FIGURE 8 Relationship between the axial stiffness and isometric force. Filled circles represent experimental data. The solid line is based on the area motor model. Bars indicate standard errors.

It might appear that the validity of the relationship between the axial stiffness and isometric force rests on Eq. 1, which already assumes a series connection. In fact, the extrapolation with Eq. 1 made the difference larger. However, that is not the case. Our conclusion is not dependent on an assumption we made. First, the force directly detected by the probe is already dependent on diamide concentration. Second, the compensation for the cell stiffness using Eq. 1 in obtaining the isometric extrapolation is the largest for untreated cells and the smallest for cells treated with the highest dose of diamide. The validity of Eq. 1 for untreated cells has been shown by using probes with various stiffnesses (Iwasa and Adachi, 1997). Thus the relationship between the axial stiffness and force generation is not the result of our assumptions.

Load-free motility

The mean value obtained for saturating amplitude of electromotility is 4.9% of the cell length for untreated cells. This value is consistent with previous reports (Ashmore, 1987; Santos-Sacchi and Dilger, 1988). For untreated cells, the midpoint of the transition is about -27 mV. The gating charge of untreated cells is 0.76e, where e is the electronic charge (Table 2). These values are also consistent with previous studies, including measurements of membrane capacitance (Santos-Sacchi, 1991; Iwasa, 1993).

The equation for describing load-free condition is obtained by setting $K_p = 0$. Equation 7 shows that saturating amplitude in the load-free condition is determined by the ratio b/K_c, both of which decrease with diamide. If we assume that the change in the modulus d_c is 6.7% at 5 mM diamide, the equation leads to a ~5% increase in the saturating amplitude in the load-free motility (Fig. 9). The magnitude of this change is not significantly affected by our assumption on the modulus d_c. We found that the model predicts a correlation between the change in amplitude and the osmotic behavior of the cell. If the ratio ϵ_c/ϵ_z during hypoosmotic perfusion is affected by the treatment more than we observed, i.e., it approaches -1 rather than our observed ratio of -1.5, the amplitude increases by ~15%.

According to the model, which does not assume changes in the motor due to diamide, the voltage of the steepest length change shifts to a more negative value when the modulus d_z decreases. This shift is the effect of reduced membrane tension due to reduced elastic moduli. The experimental shifts are larger than the predicted shifts by a factor of 10. We are inclined to think this quantitative

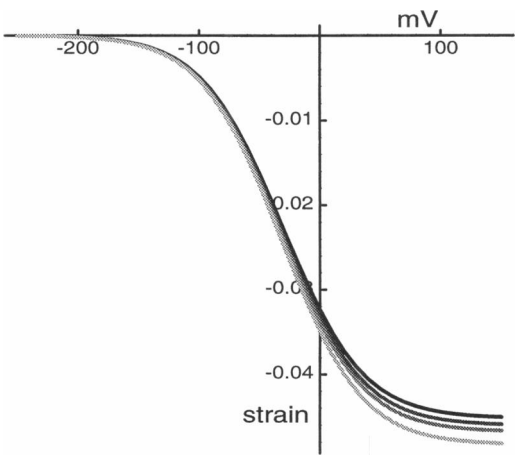

FIGURE 9 Load free displacements predicted by the area motor model. From the top (*darkest*), the axial stiffness used corresponds to control, 1 mM, 2 mM, and 5 mM (*lightest*).

difference could be related to the direct effect of diamide on the membrane motor.

Our theory predicts that the sharpness of the transition increases with reduced membrane stiffness. A reduction of the membrane area by the motor on depolarization accompanies an increase in internal pressure. An increased pressure, in turn, increases membrane tension, making the extended state of the motor less energetically favorable. This negative feedback reduces the sharpness of the membrane-potential-dependent transition. With reduced membrane stiffness, the feedback that reduced the sharpness of the transition is reduced. This should result in sharper voltage-dependent length changes. Our experimental observation seems to show that diamide reduces the sharpness parameter q^* somewhat, which is the opposite of our prediction. Because we cannot find any reason why softening of the cell membrane results in a decreased voltage sensitivity of the motor, we should accept that the reduced voltage sensitivity due to diamide is the result of a direct effect of this chemical of the motor. This direct effect may not be very unexpected, because a number of other sulfhydryl reagents reduce or even eliminate the electromotility of the OHC in the load-free condition.

We have seen earlier that the relationship between the axial stiffness and isometric force favors a series connection between the elastic element and the motor element. The relationship between the axial stiffness and the load-free amplitude, however, does not favor either a parallel or a series connection. Increasing amplitude with decreasing axial stiffness is consistent with a parallel connection. Our model, which assumes a series connection, leads to an increase in the load-free amplitude, although the effect is not as large as observed. To obtain quantitative agreement, it is possible to assume that area changes in the motor increase with diamide treatment. This assumption leads to increased amplitudes of the load-free motility and increased voltage shifts without significantly changing force production, because force production is not sensitive to area changes, as shown previously (Iwasa, 1994).

Relationship of motor function to cellular structure

Let us examine the implication of our result for our current morphological knowledge of the OHC. It is frequently assumed that the motor is the 10-nm particle in the plasma membrane (Kalinec et al., 1992; Iwasa, 1993; Huang and Santos-Sacchi, 1994; Holley, 1996). The circumferential filaments, which consist mostly of actin, are spaced at ~50-nm intervals and are connected by cross-links, made mostly of spectrin. The plasma membrane is linked to the cortical lattice by pillars at 30-nm intervals along circumferential fibers (Holley, 1996). This picture seems to indicate that the elastic element, which is dominated by the cortical lattice as evidenced by diamide sensitivity, should be in a parallel connection with the motor. A parallel connection, however, is in conflict with our observation. To avoid this problem, we can assume that a motor unit is identified not as a 10-nm particle but as a pillar, so that the connection between the motor and the elastic element could be considered to be in series. However, this interpretation has difficulty in explaining the number of motor units. While the density of the motor units in the lateral wall is similar to the density of 10-nm particles, which is 1 in ~300 nm^2, the density of pillars is 1 in ~1500 nm^2. This difference is perhaps significant. The relationship between the motile function and the detailed structure needs further elucidation.

In conclusion, diamide reduces the axial stiffness of the OHC in a dose-dependent manner. This effect is consistent with the physical picture that spectrin molecules link actin filaments, which primarily run in the circumferential direction. Our results also indicate the importance of the cortical lattice in determining the membrane elasticity. The reduction in the axial stiffness is associated with a reduction in force production in the isometric condition and with an increase in the saturating amplitude in the load-free condition. This observation is inconsistent with a parallel connection between the motor element and the diamide-sensitive elastic element, and it is consistent with a series connection. The two-state membrane motor model we used is based on a series connection and appears to be useful in sorting out changes in the elastic properties of the membrane and changes in the motor.

The authors thank Dr. Gerald Ehrenstein and Dr. Richard Chadwick for helpful comments.

REFERENCES

Ashmore, J. F. 1987. A fast motile response in guinea-pig outer hair cells: the molecular basis of the cochlear amplifier. *J. Physiol. (Lond.).* 388: 323–347.

Ashmore, J. F. 1990. Forward and reverse transduction in guinea-pig outer hair cells: the cellular basis of the cochlear amplifier. *Neurosci. Res. Suppl.* 12:S39–S50.

Becker, P. S., C. M. Cohen, and S. E. Lux. 1986. The effect of mild diamide oxidation on the structure and function of human erythrocyte spectrin, *J. Biol. Chem.* 261:4620–4628.

Bloom, M., E. Evans, and O. G. Mouritsen. 1991. Physical properties of the fluid lipid-bilayer component of cell membranes: a perspective. *Q. Rev. Biophys.* 24:293–397.

Brownell, W., C. Bader, D. Bertrand, and Y. Ribaupierre. 1985. Evoked mechanical responses of isolated outer hair cells. *Science.* 227:194–196.

Dallos, P., B. N. Evans, and R. Hallworth. 1991. Nature of the motor element in electrokinetic shape changes of cochlear outer hair cells. *Nature.* 350:155–157.

Ehrenstein, D., and K. H. Iwasa. 1996. Viscoelastic relaxation in the membrane of the auditory outer hair cell. *Biophys. J.* 71:1087–1094.

Flock, Å., B. Flock, and M. Ulfendahl. 1986. Mechanisms of movement in outer hair cells and possible structural basis. *Arch. Otorhynolaryngol.* 243:83–90.

Gale, J. E., and J. F. Ashmore. 1994. Charge displacement induced by rapid stretch in the basolateral membrane of the guinea-pig outer hair cell. *Proc. R. Soc. Lond. B.* 255:233–249.

Haest, C. W. M., D. Kamp, G. Plasa, and B. Deuticke. 1977. Intra- and intermolecular cross-linking of membrane proteins in intact erythrocytes and ghosts by SH-oxidizing agents. *Biochim. Biophys. Acta.* 469: 226–230.

Hallworth, R. 1995. Passive compliance and active force generation in the guinea pig outer hair cell. *J. Neurophysiol.* 74:2319–2328.

Hemmert, W., C. Schauz, H.-P. Zenner, and A. W. Gummer. 1997. Force generation and mechanical impedance of outer hair cells. *In* Diversity in Auditory Mechanics. E. R. Lewis, G. R. Long, R. F. Lyon, P. M. Narins, and C. R. Steele, editors. World Scientific, Singapore, 531–537.

Holley, M. C. 1996. Outer hair cell motility. *In* The Cochlea. P. Dallos, A. N. Popper, and R. R. Fay, editors. Springer, New York. 386–434.

Holley, M. C., and J. F. Ashmore. 1988. On the mechanism of a high-frequency force generator in outer hair cells isolated from the guinea pig cochlea. *Proc. R. Soc. Lond. B.* 232:413–429.

Holley, M. C., and J. F. Ashmore. 1990. Spectrin, actin, and the structure of the cortical lattice in mammalian cochlear outer hair cells. *J. Cell Sci.* 96:283–291.

Holley, M. C., F. Kalinec, and B. Kachar. 1992. Structure of the cortical lattice in mammalian cochlear outer hair cells. *J. Cell Sci.* 102:569–580.

Huang, G., and J. Santos-Sacchi. 1994. Motility voltage sensor of the outer hair cell resides within the lateral plasma membrane. *Proc. Natl. Acad. Sci. USA.* 91:12268–12272.

Iwasa, K. H. 1993. Effect of stress on the membrane capacitance of the auditory outer hair cell. *Biophys. J.* 65:492–498.

Iwasa, K. H. 1994. A membrane motor model for the fast motility of the outer hair cell. *J. Acoust. Soc. Am.* 96:2216–2224.

Iwasa, K. H. 1996. Membrane motors in the outer hair cell of the mammalian cochlea. *Comments Theoret. Biol.* 4:93–114.

Iwasa, K. H. 1997. Motor mechanisms of the outer hair cell from the cochlea. *In* Diversity in Auditory Mechanics. E. R. Lewis, G. R. Long, R. F. Lyon, P. M. Narins, and C. R. Steele, editors. World Scientific, Singapore. 580–586.

Iwasa, K. H., and M. Adachi. 1997. Force generation in the outer hair cell from the cochlea. *Biophys. J.* 73:546–555.

Iwasa, K. H., and R. S. Chadwick. 1992. Elasticity and active force generation of cochlear outer hair cells. *J. Acoust. Soc. Am.* 92: 3169–3173.

Kachar, K., E. B. Brownell, R. Altschuler, and J. Fex. 1986. Electrokinetic shape changes of cochlear outer hair cells. *Nature.* 322:365–367.

Kakehata, S., and J. Santos-Sacchi. 1995. Membrane tension directly shifts voltage dependence of outer hair cell motility and associated gating charge. *Biophys. J.* 68:2190–2197.

Kalinec, F., M. C. Holley, K. H. Iwasa, D. J. Lim, and B. Kachar. 1992. A membrane-based force generation mechanism in auditory sensory cells. *Proc. Natl. Acad. Sci. USA.* 89:8671–8675.

Kalinec, F., and B. Kachar. 1993. Inhibition of outer hair cell electromotility by sulfhydryl specific reagents. *Neurosci. Lett.* 157:231–234.

Kalinec, F., and B. Kachar. 1995. Structure of the electromechanical transduction mechanism in mammalian outer hair cells. *In* Active Hearing. Å. Flock, D. Ottoson, and M. Ulfendahl, editors. Pergamon, London. 181–193.

Knipper, M., U. Zimmermann, I. Kopschall, K. Rohbock, S. Jungling, and H. P. Zenner. 1995. Immunological identification of candidate proteins involved in regulating active shape changes of outer hair cells. *Hear. Res.* 86:100–110.

Kojima, H., A. Ishijima, and T. Yanagida. 1994. Direct measurement of stiffness of single actin filaments with and without tropomyosin by in vitro nanomanipulation. *Proc. Natl. Acad. Sci. USA.* 91:12962–12966.

Kosower, N. S., and E. M. Kosower. 1995. Diamide: an oxidant probe for thiols. *Methods Enzymol.* 251:123–133.

Maeda, N., K. Kon, K. Imaizumi, M. Sekiya, and T. Shiga. 1983. Alteration of rheological properties of human erythrocytes by crosslinking of membrane proteins. *Biochim. Biophys. Acta.* 735:104–112.

Mammano, F., and J. F. Ashmore. 1993. Reverse transduction measured in the isolated cochlea by laser Michelson interferometry. *Nature.* 365: 838–841.

Mountain, D. C. 1980. Changes in endolymphatic potential and crossed olivocochlear bundle stimulation alter cochlear mechanics. *Science.* 210: 71–72.

Nishida, Y., T. Fujimoto, A. Takagi, I. Honjo, and K. Ogawa. 1993. Fodrin is a constituent of the cortical lattice in outer hair cells of the guinea pig cochlea: immunocytochemical evidence. *Hear. Res.* 65:274–280.

Santos-Sacchi, J. 1991. Reversible inhibition of voltage-dependent outer hair cell motility and capacitance. *J. Neurosci.* 11:3096–3110.

Santos-Sacchi, J., and J. P. Dilger. 1988. Whole cell currents and mechanical responses of isolated outer hair cells. *Hear. Res.* 35:143–150.

Tolomeo, J. A., and C. R. Steele. 1995. Orthotropic piezoelectric properties of the cochlear outer hair cell wall. *J. Acoust. Soc. Am.* 97:3006–3011.

Xue, S., D. C. Mountain, and A. E. Hubbard. 1993. Direct measurement of electrically-evoked basilar membrane motion. *In* Biophysics of Hair Cell Sensory Systems. H. Duifhuis, J. W. Horst, P. van Dijk, and S. van Netten, editors. World Scientific, Singpore. 361–368.

Xue, S., D. C. Mountain, and A. E. Hubbard. 1995. Electrically evoked basilar membrane motion. *J. Acoust. Soc. Am.* 97:3030–3041.

Zajic, G., and J. Schacht. 1991. Shape changes in isolated outer hair cells: measurements with attached microspheres. *Hear. Res.* 52:407–410.